Chapter 2

Defibrillation and Cardiac Geometry

Dan Blendea, Razvan Dadu and Craig A. McPherson

Additional information is available at the end of the chapter

http://dx.doi.org/10.5772/55120

1. Introduction

Although ICD therapy is an efficient and reliable therapeutic method, internal defibrillation is a traumatic experience; moreover and there is accumulating evidence that internal defibrillation, especially with high defibrillation energy, may adversely affect cardiac function and even patient prognosis [1, 2]. Therefore, considerable research efforts have been focused on better defining defibrillation mechanisms, particularly aiming at and improving defibrillation efficacy and in order to reduce lowering defibrillation energy requirements.

Recent developments in cardiac simulation have been used to create more accurate defibrillation models. The chapter tries to focus on the importance of geometry in the different defibrillation models, and explores potential applications of these models to improve the transvenous defibrillation systems, and the more recently developed extracardiac ICDs.

2. Geometry and pathogenesis of ventricular fibrillation

The exact mechanism of ventricular fibrillation (VF) is still unknown. One of the most accepted hypotheses is that during VF, synchronous contraction of the muscle is disrupted by fast, vortex-like, rotating waves of electrical activity named rotors.[3-6]. The spiral wave rotates about an organizing center, or core, which is thought to be an unexcited but excitable medium that defines the primary dynamic characteristics of the wave. At the core of the vortex is a line of phase singularities (i.e. a region where the phase is undefined) named filament. It seems that, at least in the initial phases, a relatively stable circuit, called the mother rotor, maintains VF.[7] Zaitsev et al[7] used the term domain to define a region in which all of the tissue has the same peak frequency in the VF power spectrum.[8] Optical recordings during VF found that a single domain of highest peak frequency was present, named the dominant domain, and

was surrounded by domains of lower peak frequencies. Some wavefronts that arouse in the dominant domain propagate into domains with lower peak frequencies, and others block at the boundary between domains.[9] These findings suggest that that VF is maintained by a single, stationary, stable reentrant circuit, i.e., the mother rotor, in the dominant domain, which has the shortest refractory period from which activations propagate into the more slowly activating domains with longer refractory periods. Nanthakumar et al [10] demonstrated reentrant wavefronts in human VF, providing a direct demonstration of phase singularities, wavebreaks and rotor formation in severely diseased, explanted human hearts.[11] Importantly, they found also wavefronts as large as the entire vertical length of the optical field, which suggested a high degree of organization.[10] Findings from simultaneous epicardial and endocardial multielectrode mapping in patients with cardiomyopathy [12] suggested that during induced VF episodes, stable reentrant wavefronts occur in the endocardium and the epicardium. The same authors demonstrated a stable source in the endocardium, with a highly organized pattern in the local electrogram and a simultaneous and disorganized pattern in the epicardium, consistent with the hypothesis of 3-dimensional scroll waves.[12] Thus, the short-lived rotors on the epicardial and/or endocardial surfaces are thought to be manifestations of a scroll wave organized along the fiber orientation within the wall. Massé et al also observed variable block patterns in wavefront transmission, resulting in disorganized activity and wavefront fragmentation.[12] Rotors may exist alone as stationary high-frequency mother rotors that generate wavefronts that fractionate and disorganize in its periphery. They may also manifest as drifting rotors or even as rotors that rapidly die off leaving multiple offspring wavelets that originate new short-lived rotors and new wavelets.[11]

3. Rotors and heart geometry

Rotors are common to many biological, chemical and physical excitable media and their dynamics have been researched intensively. The specific anatomical structure of the cardiac chambers is likely to be a crucial factor in determining the fibrillatory behavior. The heterogeneity of the ventricular anatomy is likely to play an important role in rotor dynamics. For example, the thicker left ventricular wall may manifest the complex dynamics of 3-dimensional scroll waves much more readily than the thinner right ventricle and the atrial walls. There is a left-to-right gradient of dominant frequencies, suggesting that the left heart may be playing the leading role in maintaining fibrillation. [11] Kim et al. suggested that sink-to-source mismatch between areas with different thickness in the ventricle may serve to anchor rotors [13] and these rotors may span the thickness of the ventricular wall. For instance, the papillary muscles in the LV may help to stabilize rotors.[11,14]

A thickness threshold is sought at which complex and changing short-period wave behavior abruptly becomes more organized into simple drifting spiral waves of slightly longer period. [15 16] Such a threshold was indeed found in canine ventricles and bears the same relation to rotor period and representing about $1/\pi$ times the distance a spiral wave propagates during one rotation period.[16] This distance is the nominal diameter of the rotor, the source of the reentrant activation front. In three dimensions, this source is not, as in two dimensions, a small

elliptical disk but a filament.[16] If the myocardial tissue is thick enough to admit a vortex filament lying on its side, the rotor can move more freely, fragment, and close in rings.[16] In numerical experiments with uniformly anisotropic and perfectly continuous and homogeneous three-dimensional excitable media, such vortex filaments spontaneously lash about unless confined to a layer thinner than about a rotor diameter.[16] Apart from reasonably steady rotation, their motion is apparently irregular. It seems that there is a thickness threshold of about one rotor diameter (3 to 10 mm, depending on fiber orientation) that complements the known area threshold for creating and sustaining a rotor (3 mm by 3 or 10 mm perpendicular to thickness, depending on fiber orientation). Together, they constitute a compact critical volume of 3 mm by 3 mm by 10 mm (about 0.1 g of tissue) beyond which reentrant tachycardia (monomorphic or polymorphic) can spontaneously become more complex (fibrillation).[16] Another finding suggesting role of tissue thickness for development of ventricular fibrillation is the observation that rotors in situ have a longer period in thinner (and more epicardial) layers.[17] Another possible contributor to the thickness effect arises from the conspicuous rotation of fiber orientation from epicardium to endocardium. It has been suggested that twist renders vortex filaments unstable.[18] There is a suggestion that thicker myocardium, bearing less twist per unit distance, would be less liable to such instabilities. The thinner right ventricular free wall is capable of supporting spiral waves more stably, and the thicker left ventricular wall more often degenerates to fibrillation. [16,19]

An interesting analysis that gives more insight into the pathogenesis of rotor is a correlation of body size, heart weight, ventricular surface area, and wall thickness in different mammalians against the minimum safely sustainable sinus rhythm interval over different species. This analysis assumes that the rotor dynamics is the same in the ventricular myocardium of different mammalian species.[16] Data from mammals including rats, guinea pigs, and man shows that rotors thus turn out to lie on the phylogenetic trend line near the transition from normal hearts that spontaneously defibrillate to normal hearts capable of sustained fibrillation. It seems that ventricles cannot stably beat faster than the rotor period unless they are too small to accommodate a rotor. Individuals susceptible to death by ventricular fibrillation have sufficient ventricular surface dimensions to accommodate a rotor pair (I to 2 cm in longitudinal fiber direction) and have a wall thickness sufficient to accommodate a vortex filament of one rotor diameter [transverse to fibers, with anisotropically reduced electrical scale, about (1 cm)/3 = 3 to 4 mm.[16] Structural remodeling has been shown to interfere with rotor behavior. With regards to the ventricles, it has been shown experimentally that the dynamics of VF in the presence of heart failure are different from those in the normal heart. Heart failure remodeling decreases VF rate and increases VF organization.[11]

4. Geometry and defibrillation

The only clinically effective method for eliminating vortices in the heart is the delivery of a high-energy electric shock that depolarizes and also hyperpolarizes the tissue with a voltage gradient of about 5 V/cm.[6] In the bidomain representation, the voltage in cardiac tissue is the potential drop between the intracellular and extracellular medium. Theory predicts [20] that,

in the presence of an electric field, discontinuities in tissue conductivity, such as blood vessels, changes in fiber direction, fatty tissue and intercellular clefts, induce a redistribution of intracellular and extracellular currents that can locally hyperpolarize or depolarize the cells. At the depolarization threshold, an excitation wave is emitted.[6,20,21] Conceptually, defibrillation can be considered to be a two-step process. Firstly, the applied shock drives currents that traverse the myocardium and cause complex polarization changes in transmembrane potential distribution. Secondly, post-shock active membrane reactions are invoked that eventually result either in termination of ventricular fibrillation in the case of shock success, or in reinitiation of fibrillatory activity in the case of shock failure.[22]

Over a decade ago, bidomain simulations[23] followed by optical mapping studies [24,25] demonstrated that the membrane response in the vicinity of a strong unipolar stimulus involved simultaneous occurrence of positive (depolarizing) and negative (hyperpolarizing) effects in close proximity. This finding of 'virtual electrodes' was in contrast with the established view [26] that tissue responses should only be depolarizing (hyperpolarizing) if the stimulus was cathodal (anodal).[27] Essentially, the virtual electrode polarization (VEP) theory states that adjacent areas of opposite polarizations exist around the tip of the pacing electrode.[28] Sepulveda et al. [23] showed that the region depolarized (excited) by a strong stimulus has a dog-bone shape, with its long axis perpendicular to the direction of the myocardial fibers. Regions of hyperpolarization (called virtual anodes) exist adjacent to the electrode along the fiber direction. A virtual anode is an example of a virtual electrode. Many researchers have observed these regions of depolarization and hyperpolarization experimentally. [25,29] Depolarization can excite a cell and conversely, hyperpolarization can de-excite a cell. The cellular response to shock-induced VEP depends on the strength and polarity of the shock, as well as on the electrophysiological state of the cell at the time of shock delivery. Positive VEP can result in regenerative depolarization in regions where tissue is at or near diastole; such activation is termed 'make' because it takes place at the onset (make) of the shock. A strong negative VEP can completely abolish the action potential (i.e. regenerative repolarization), thus creating post-shock excitable gaps in the virtual anode regions. The close proximity of a de-excited region and a virtual cathode has been shown, in both modelling studies and optical mapping experiments,[25] to result in an excitation at shock end (termed 'break' excitation, i.e. at the break of the shock). The virtual cathode serves as an electrical stimulus eliciting a regenerative depolarization and a propagating wave in the newly created excitable gap.[27] For a defibrillation shock to succeed, it must extinguish existing VF activations throughout the myocardium (or in a critical mass of it), as well as not initiate new fibrillatory wavefronts.[27] A shock succeeds in extinguishing fibrillatory wavefronts and not initiating new re-entry if make/break excitations manage to traverse the shock-induced excitable gaps before the rest of the myocardium recovers from shock-induced depolarization.[27] Defibrillation failure has been explained by one (or both) of the following mechanisms: (I) the shock fails to extinguish all or a sufficient amount of fibrillatory electrical activity and (2) newly created shock-induced wavebreaks by near-threshold stimulating fields occurring at existing excitable gaps.[30]

Detailed analysis of VEP etiology demonstrated that both applied field [24] and tissue structure are major determinants of the shape, location, polarity and intensity of the shock-induced polarization.[24,27] The cellular response to shock-induced VEP depends on the strength and polarity of the shock, as well as on the electrophysiological state of the cell at the time of shock delivery.[27] There is a relationship between the response of the tissue to an electric field and the spatial distribution of heterogeneities in the scale-free coronary vascular structure. In response to a pulsed electric field, these heterogeneities serve as nucleation sites for the generation of intramural electrical waves that can generate tissue depolarization. These intramural wave sources permit targeting of electrical turbulence near the cores of the vortices of electrical activity that drive complex fibrillatory dynamics. Simultaneous and direct access to multiple vortex cores results in rapid synchronization of cardiac tissue and therefore, efficient termination of fibrillation. Using this control strategy, Luther et al. demonstrated low-energy termination of fibrillation in vivo. Their results give new insights into the mechanisms and dynamics underlying the control of spatio-temporal chaos in heterogeneous excitable media and provide new research perspectives towards alternative, life-saving low-energy defibrillation techniques.[6]

5. Geometry and lead positioning for cardiac defibrillation

Most models used to describe defibrillation view the myocardial mass as an isotropic conductive domain and use the critical mass hypothesis to define successful defibrillation. According to this hypothesis the success of a defibrillation shock depends on rendering a critical mass of the myocardium inexcitable, such that fibrillation wavefronts have no myocardium to depolarize and propagate through.[19] It has been found that raising the extracellular potential gradient above a critical level renders myocardium refractory.[31] Frazier et al.[32] have found the critical level of potential gradient to be close to 5 V/cm, and a commonly accepted value for critical myocardial mass is 95%. [33]

In a recent study Yang et al. examined the effect of coil position on active-can single-coil ICD defibrillation efficacy by using a finite difference thoracic model which incorporated realistic geometries and conductive inhomogeneities of human thoracic tissues. [34] Four electrode configurations with the coil placed, respectively, in the right ventricular (RV) apex, in the middle of RV cavity, along the free wall in RV, or along the septal wall in RV, were simulated and their defibrillation efficacies were evaluated based on a set of metrics including voltage defibrillation threshold (VDFT) and current defibrillation threshold. It was found that the optimal electrode configuration is to position the coil in the middle of the RV cavity.

The RV cavity-to-can configuration had more endocardium exposed to the more uniform and relatively high voltage gradient fields. Other configurations exposed only endocardic surfaces near the electrodes to high voltage gradient fields and the voltage gradient drops more quickly in myocardial tissue as its resistivity value is one-third larger than blood's.

Aguel et al[35] used a high-resolution finite element model of a human torso that includes the fiber architecture of the ventricular myocardium to find the role of lead positioning in a

transvenous lead-to-can defibrillation electrode system. They found that, among single lead systems, posterior positioning of leads in the right ventricle lowers VDFTs. Furthermore, a septal location of leads resulted in lower VDFTs than free-wall positioning. Increasing the number of leads, and thus the effective lead surface area in the right ventricle also resulted in lower VDFTs. However, the lead configuration that resulted in the lowest VDFTs is a combination of mid-cavity right ventricle lead and a mid-cavity left ventricle lead.

Since the shape of the myocardial mass–voltage gradient curve is determined entirely by the geometry of the model and the lead design,[35] an improvement in defibrillation efficacy may be achieved by adjustment of the defibrillation lead surface and position, as this allows a more even distribution of the voltage gradient field over a wider surface of the myocardium.[36] Although centering the coils inside the heart chambers is probably not feasible with the current leads, positioning the coil in the middle of the RV cavity functioned equivalently in this sense as it had almost the entire RV endocardial surface exposed to a relatively evenly distributed voltage gradient field considering blood's resistivity is significantly less than the resistivity value of myocardium.

Current density distribution is another important parameter to use in evaluating the efficacy of defibrillation. The cross-sectional current density distribution showed that in the full tissue model skeletal muscle provided an alternative pathway for the current flow. By calculating the current flowing through various regions in the cross-sections it was found that more than 25% of the total current passing through the cross-sections flowed through the skeletal muscle around the outer boundary of the thorax, independent of electrode configuration. On average, 10% of the current was shunted through the relatively high resistivity fat on the outer boundaries of the thorax and another 10% was shunted though the left lung. This suggests that the amount of skeletal muscle, fat and lungs impact the amount of current reaching the heart. This finding is consistent with the results reported by Geddes et al.[37] that indicates body size or shape has a significant influence on the amount of current required for successful defibrillation, though it was based on studies of transthoracic ventricular defibrillation. Examining the current flowing through the heart in the cross-sections on the average, less than 10% of the current flowed through the myocardium, and a major portion of the current flowing through the heart region was shunted through the blood chambers.[34] In a simplified view, the current from the electrode in the RV can propagate up through the blood chambers to the base of the heart, great vessels, and lung to the can, or out through the myocardial wall to the skeletal muscle and up to the can. Both paths are used, but as the ventricles become more enlarged as in patients with advanced heart failure, the low resistivity blood shifts more current up through the base of the heart and away from the skeletal muscle.[34] This would suggest that the large heart chambers of patients in heart failure, or with an enlarged heart, would tend to shunt the current away from the myocardial tissue in the middle regions of the heart, thus resulting in the need for higher defibrillation currents.[34]

5.1. Clinical aspects of right ventricular lead positioning for defibrillation

Until relatively recently lead placement in the RV apex has been the standard of care for patients requiring pacemaker or defibrillator lead placement (Figure 1).[38]

http://dx.doi.org/10.5772/55120

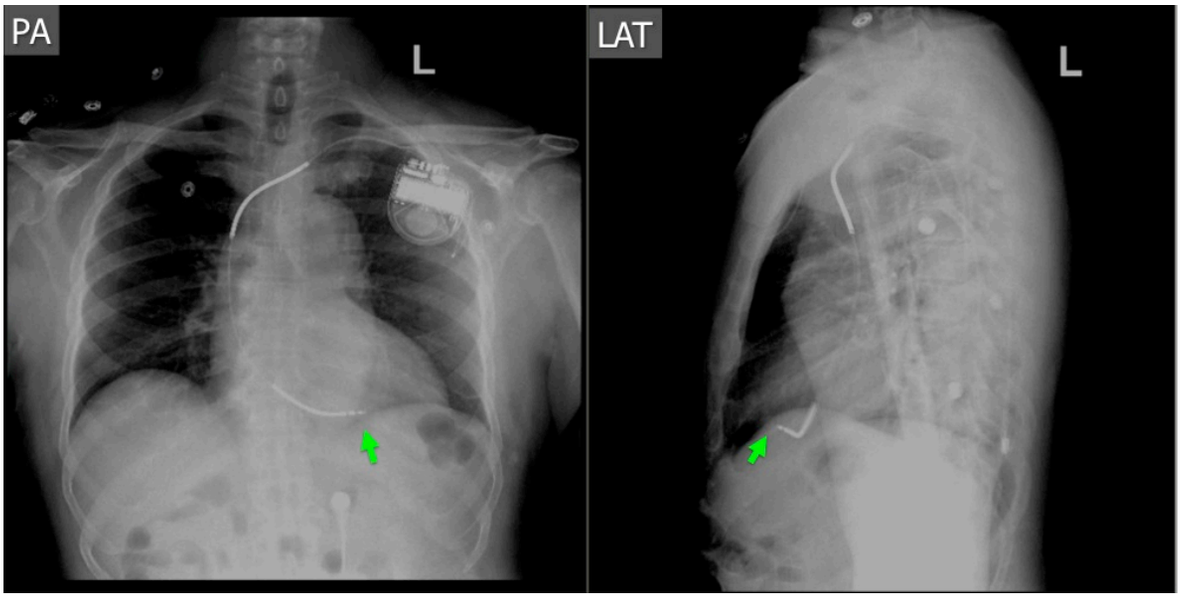

Figure 1. Single chamber dual coil ICD system with the lead placed in the apex of the right ventricle (arrow). Postero-anterior (PA) and lateral (LAT) radiographic views.

It was advised to place the RV coil towards the apex to reduce the DFTs, mainly driven by data obtained before the active can configurations were introduced.[38] Without the hot can pulling current toward the apex, it was important to have the RV coil tip deep in the apex. Otherwise, the current would tend to follow the blood pool back to the SVC coil, shunting the defibrillation energy away from the LV myocardium and raising the VDFT. [38] With a chest electrode ("hot can") in place, the RV apical position is not as critical because current is pulled directed from whatever position in the RV that the coil resides, through the apex to the pectoralis major muscle and to the hot can, thereby including the LV myocardium in the wave front's path.[39] Actually with a hot can, and with no SVC coil, the apical position was shown to be inferior in terms of DFTs.[34] If a hot can and an SVC coil are used the data available seems to suggest a slight advantage for the RV apex position. Clinical studies comparing the DFT for an RV coil tip in the apex versus in the right ventricular outflow tract using biphasic waveforms and a hot can showed that the mean benefit of an apical position was approximately 10% DFT reduction.[38,40,41] This relatively small benefit must be weighed against the increased risk of perforation associated with apical lead positioning.[38,42] Based on the current data the best compromise position of the RV coil tip seems to be along the septum midway (Figure 2) between the apex and RVOT (Figure 3).

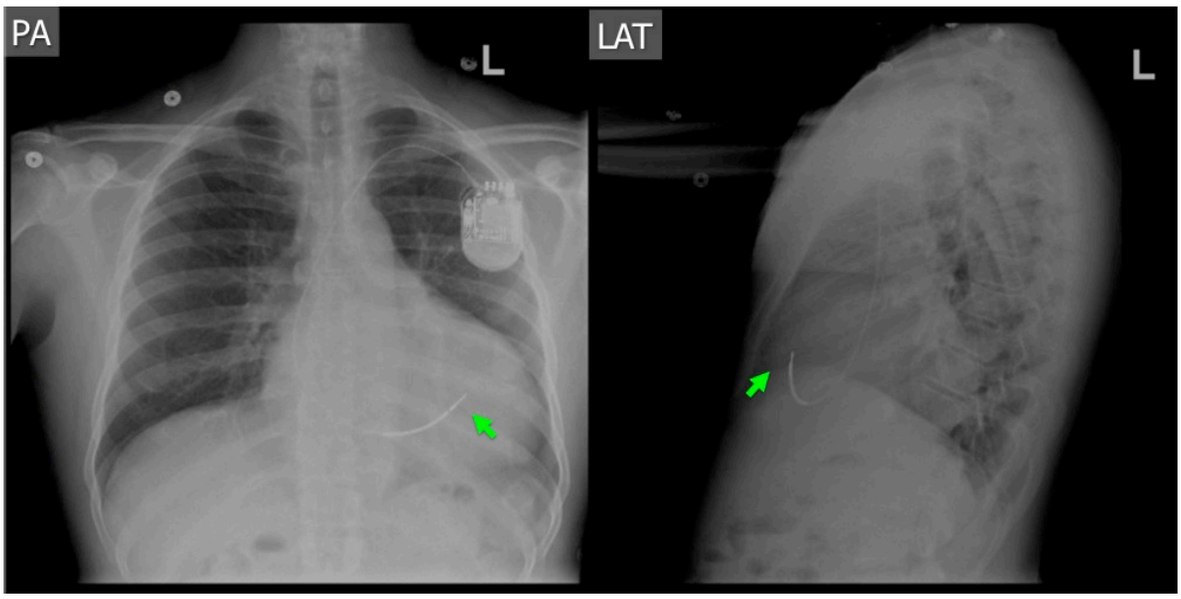

Figure 2. Single-chamber single-coil ICD system with the lead placed in a mid-septal location (arrow). Postero-anterior (PA) and lateral (LAT) radiographic views.

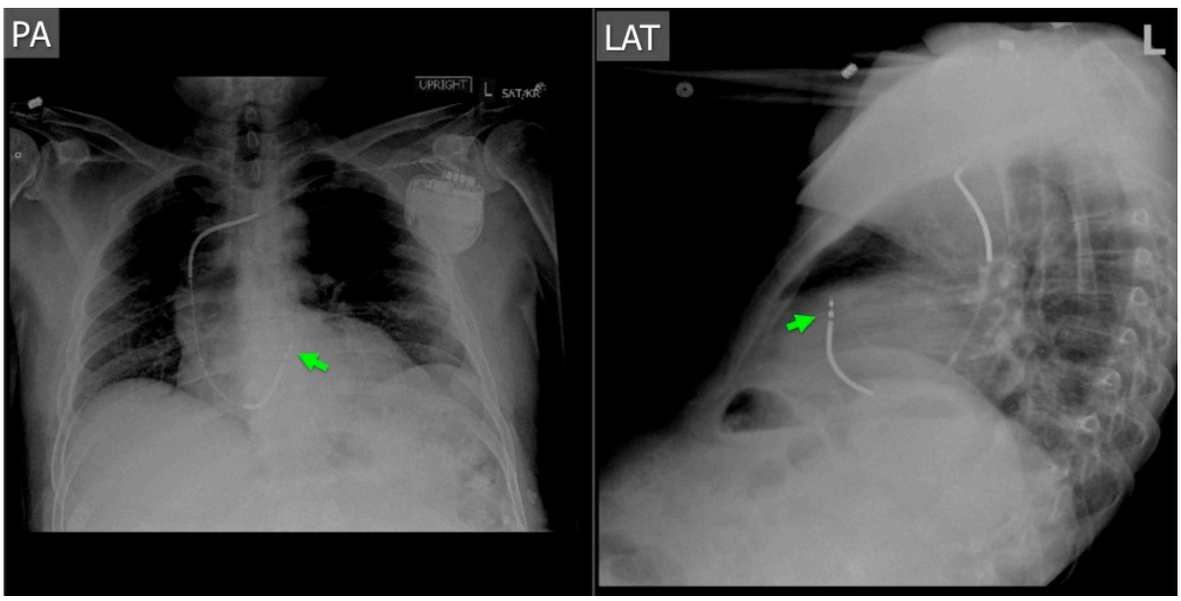

Figure 3. Single-chamber dual-coil ICD system with the lead placed at the base of the right ventricular outflow tract (arrow). Postero-anterior (PA) and lateral (LAT) radiographic views.

If the SVC coil is used, (given the lower DFTs for the mid-septal/RVOT position) an apical or apical-septal position may be considered (Figure 1). If the SVC coil is not used, the mid-septal location (Figure 2) appears to give lower DFTs than the apical tip location according to a modeling study.[34,38]

The effect of waveform polarity has been studied using both monophasic and biphasic waveforms, and the available data shows 15-20% DFT mean reduction when an anodal RV coil configuration is being used. [38,43] These results are predicted by the virtual electrode hypothesis of defibrillation[44] that predicts that post-shock virtual electrodes launch new wavefronts toward the anode.[38] A right ventricular cathode produces expanding, pro-arrhythmic wavefronts, whereas a right ventricular anode produces collapsing, self-extinguishing wavefronts. [38] An additional beneficial effect of anodal RV shocks may be to increase the homogeneity of membrane time constants in comparison with cathodal shocks.[38,45]

Another element of lead technology that can affect the efficiency of a defibrillation system is the SVC coil. Studies on patients with active-can lead configurations suggest that the addition of the SVC coil decreases the DFT and reduces impedance. With an apically placed RV coil and a prepectoral hot can, major current flow is to the pectoralis major and to the ICD can. Minimal current flows to the posterior base. The addition of an SVC coil directs some current vertically and toward the posterior.

There are several detrimental effects from the use of the SVC coil, especially for a coil placed in the right atrium. The low SVC coil diverts current from the apex and LV free wall because the RV and atrial blood pool provide a lower resistance path. In addition, a low cathodal SVC coil could launch wavefronts into basal RV. And, additionally, the extraction of a dual-coil lead is much more challenging because the adherences that can form between the SVC coil and the venous wall.[38]

A recent study analyzed comparatively the DFTs for active and inactive SVC coils.[46] The results depended on the single coil impedance. If the single coil impedance was >58Ω, then an active SVC coil almost always lowered the DFT. If the single coil impedance was already in the normal range (<58 Ω), then the effect of the SVC coil was split.[38] Half of patients had a lower DFT and half had a higher DFT. Interestingly, if the SVC coil was active, its position was important: an SVC coil in the SVC/right atrial junction increased the DFT, and an SVC coil placed in the SVC/ innominate junction decreased the DFT.[46]

6. Electrode configurations for subcutaneous ICDs

Total subcutaneous implantable subcutaneous defibrillators (S-ICDs) have been developed as alternative ICD strategies allowing more widespread application of ICD therapy for the primary prevention of sudden death. The optimal device and electrode configurations for S-ICDs are not well known. Image-based defibrillation finite element models have been used to predict the myocardial electric field generated during defibrillation shocks in a variety of subcutaneous electrode positions, in order to determine factors affecting optimal lead positions for subcutaneous ICDs (S-ICD), and ultimately to improve the efficacy of these defibrillation systems.

Jolley et al.[47] used image-based finite element models (FEM) to predict the myocardial electric field generated during defibrillation shocks (pseudo-DFT) in a wide variety of subcutaneous electrode positions to determine factors affecting optimal lead positions for subcutaneous implantable cardioverter-defibrillators (S-ICD). An image-based FEM of an adult man was used to predict pseudo-DFTs across a wide range of technically feasible S-ICD electrode placements. Generator location, lead location, length, geometry and orientation, and spatial relation of electrodes to ventricular mass were systematically varied. Best electrode configurations were determined, and spatial factors contributing to low pseudo-DFTs were identified using regression and general linear models.[47] One previously published and validated S-ICD configuration[48] was selected as the base case for normalization of the predicted DFTs of all tested configurations. This is the system proposed by Lieberman et al[48], which uses a low, medial pectoral position of an active generator and a 25-cm posterolateral electrode extending around the back of the left thorax between the 6th and 10th intercostal space, extending the tip as close to the spine as possible.

The study by Jolley and colleagues revealed that a wide variety of conceivable electrode orientations, some of them quite unusual and not previously reported, were predicted to be as effective or more effective than the base case (pseudo-DFT ratio <=1).[47] Univariate modeling results suggested that a variety of anatomical factors affecting the geometry of system configuration influenced pseudo-DFT. Placement of the generator in the parasternal position was more efficient than more lateral and remote positions (mid-clavicular, anterior-axillary, abdominal). Anterolateral and posterior electrode positions were better than para-sternal, and anterolateral better than anterior. Right-sided generators were more efficient than left-sided generators, whereas the converse was true for electrode laterality. Although some of these alternatives represent simple modifications of the previously proposed system, many involve changes in lead design and implant technique that are substantial; in particular, the contralateral placement of generator and lead.

Multivariate modeling using linear regression models showed that favorable alignment of shock vector with ventricular myocardium, increased lead length, can horizontal position, contralateral lead-generator position, and distance of can from the heart independently predicted pseudo-DFTs. The relative positions of the generator, the lead(s), and the ventricular myocardium accounted for nearly half of the predicted variability in the pseudo-DFT. This reflects the intuitive observation that electrodes should be positioned to place the heart as nearly between them as possible. This multivariate analysis revealed important principles that may guide the design of subcutaneous ICDs. Placement of the electrodes to align the inter-electrode shock vector as closely as possible to the center of mass of the ventricular myocar-dium, and use of longer electrode coil lengths are associated with lower DFTs and account for the majority of variability of this parameter. Manipulation of electrode length contributed almost 25% of the variability in pseudo-DFTs, with decreases in pseudo-DFTs predicted with extension of coil length from 5 to 10 cm and longer. Neither of these factors has previously been quantified for subcutaneous electrode placement and may prove useful in determining optimal orientations. Notably, although electrode arrays were often identified as useful in many efficient configurations, the use of an array was generally not necessarily more efficient than a single electrode of equal length similarly positioned. This finding implies both for S-

ICD design and for current subcutaneous arrays used to augment transvenous systems with unacceptably high DFTs that a simple, single-electrode system is likely to offer as much benefit as an array, which is more difficult to implant and may be more prone to failure.

Author details

Dan Blendea[1], Razvan Dadu[2] and Craig A. McPherson[2]

1 Massachusetts General Hospital - Harvard Medical School, USA

2 Bridgeport Hospital – Yale University School of Medicine, USA

References

[1] Poole, J. E, Johnson, G. W, Hellkamp, A. S, et al. Prognostic importance of defibrillator shocks in patients with heart failure. N Engl J Med (2008). , 359, 1009-17.

[2] Blendea, D, Blendea, M, Banker, J, & Mcpherson, C. A. Troponin T elevation after implanted defibrillator discharge predicts survival. Heart (2009). , 95, 1153-8.

[3] Davidenko, J. M, Pertsov, A. V, Salomonsz, R, Baxter, W, & Jalife, J. Stationary and drifting spiral waves of excitation in isolated cardiac muscle. Nature (1992). , 355, 349-51.

[4] Gray, R. A, Pertsov, A. M, & Jalife, J. Spatial and temporal organization during cardiac fibrillation. Nature (1998). , 392, 75-8.

[5] Witkowski, F. X, Leon, L. J, Penkoske, P. A, et al. Spatiotemporal evolution of ventricular fibrillation. Nature (1998). , 392, 78-82.

[6] Luther, S, Fenton, F. H, Kornreich, B. G, et al. Low-energy control of electrical turbulence in the heart. Nature (2011). , 475, 235-9.

[7] Zaitsev, A. V, Berenfeld, O, Mironov, S. F, Jalife, J, & Pertsov, A. M. Distribution of excitation frequencies on the epicardial and endocardial surfaces of fibrillating ventricular wall of the sheep heart. Circ Res (2000). , 86, 408-17.

[8] Tabereaux, P. B, Dosdall, D. J, & Ideker, R. E. Mechanisms of VF maintenance: wandering wavelets, mother rotors, or foci. Heart Rhythm (2009). , 6, 405-15.

[9] Samie, F. H, Berenfeld, O, Anumonwo, J, et al. Rectification of the background potassium current: a determinant of rotor dynamics in ventricular fibrillation. Circ Res (2001). , 89, 1216-23.

[10] Nanthakumar, K, Jalife, J, Masse, S, et al. Optical mapping of Langendorff-perfused human hearts: establishing a model for the study of ventricular fibrillation in humans. Am J Physiol Heart Circ Physiol (2007). H, 875-80.

[11] Vaquero, M, Calvo, D, & Jalife, J. Cardiac fibrillation: from ion channels to rotors in the human heart. Heart Rhythm (2008). , 5, 872-9.

[12] Masse, S, Downar, E, Chauhan, V, Sevaptsidis, E, & Nanthakumar, K. Ventricular fibrillation in myopathic human hearts: mechanistic insights from in vivo global endocardial and epicardial mapping. Am J Physiol Heart Circ Physiol (2007). H, 2589-97.

[13] Kim, Y. H, Yashima, M, Wu, T. J, Doshi, R, Chen, P. S, & Karagueuzian, H. S. Mechanism of procainamide-induced prevention of spontaneous wave break during ventricular fibrillation. Insight into the maintenance of fibrillation wave fronts. Circulation (1999). , 100, 666-74.

[14] Wu, T. J, Lin, S. F, Baher, A, et al. Mother rotors and the mechanisms of D600-induced type 2 ventricular fibrillation. Circulation (2004). , 110, 2110-8.

[15] Winfree, A. T. Scroll-shaped waves of chemical activity in three dimensions. Science (1973). , 181, 937-9.

[16] Winfree, A. T. Electrical turbulence in three-dimensional heart muscle. Science (1994). , 266, 1003-6.

[17] Kavanagh, K. M, Kabas, J. S, Rollins, D. L, Melnick, S. B, Smith, W. M, & Ideker, R. E. High-current stimuli to the spared epicardium of a large infarct induce ventricular tachycardia. Circulation (1992). , 85, 680-98.

[18] Panfilov, A. V, & Keener, J. P. Generation of reentry in anisotropic myocardium. J Cardiovasc Electrophysiol (1993). , 4, 412-21.

[19] Zipes, D. P, Fischer, J, & King, R. M. Nicoll Ad, Jolly WW. Termination of ventricular fibrillation in dogs by depolarizing a critical amount of myocardium. Am J Cardiol (1975). , 36, 37-44.

[20] Plonsey, R. The nature of sources of bioelectric and biomagnetic fields. Biophys J (1982). , 39, 309-12.

[21] Fast, V. G, Rohr, S, Gillis, A. M, & Kleber, A. G. Activation of cardiac tissue by extracellular electrical shocks: formation of'secondary sources' at intercellular clefts in monolayers of cultured myocytes. Circ Res (1998). , 82, 375-85.

[22] Trayanova, N, Constantino, J, Ashihara, T, & Plank, G. Modeling defibrillation of the heart: approaches and insights. IEEE Rev Biomed Eng (2011). , 4, 89-102.

[23] Sepulveda, N. G, Roth, B. J, & Wikswo, J. P. Jr. Current injection into a two-dimensional anisotropic bidomain. Biophys J (1989). , 55, 987-99.

[24] Knisley, S. B, Trayanova, N, & Aguel, F. Roles of electric field and fiber structure in cardiac electric stimulation. Biophys J (1999). , 77, 1404-17.

[25] Wikswo, J. P. Jr., Lin SF, Abbas RA. Virtual electrodes in cardiac tissue: a common mechanism for anodal and cathodal stimulation. Biophys J (1995). , 69, 2195-210.

[26] Hodgkin, A. L, & Rushton, W. A. The electrical constants of a crustacean nerve fibre. Proc R Soc Med (1946). , 134, 444-79.

[27] Trayanova, N. Defibrillation of the heart: insights into mechanisms from modelling studies. Exp Physiol (2006). , 91, 323-37.

[28] Sambelashvili, A. T, Nikolski, V. P, & Efimov, I. R. Virtual electrode theory explains pacing threshold increase caused by cardiac tissue damage. Am J Physiol Heart Circ Physiol (2004). H, 2183-94.

[29] Knisley, S. B, Hill, B. C, & Ideker, R. E. Virtual electrode effects in myocardial fibers. Biophys J (1994). , 66, 719-28.

[30] Efimov, I. R, Gray, R. A, & Roth, B. J. Virtual electrodes and deexcitation: new insights into fibrillation induction and defibrillation. J Cardiovasc Electrophysiol (2000). , 11, 339-53.

[31] Lepeschkin, E, Jones, J. L, Rush, S, & Jones, R. E. Local potential gradients as a unifying measure for thresholds of stimulation, standstill, tachyarrhythmia and fibrillation appearing after strong capacitor discharges. Adv Cardiol (1978). , 21, 268-78.

[32] Frazier, D. W, Wolf, P. D, Wharton, J. M, Tang, A. S, Smith, W. M, & Ideker, R. E. Stimulus-induced critical point. Mechanism for electrical initiation of reentry in normal canine myocardium. J Clin Invest (1989). , 83, 1039-52.

[33] Ideker, R. E, Wolf, P. D, Alferness, C, Krassowska, W, & Smith, W. M. Current concepts for selecting the location, size and shape of defibrillation electrodes. Pacing Clin Electrophysiol (1991). , 14, 227-40.

[34] Yang, F, & Patterson, R. Optimal transvenous coil position on active-can single-coil ICD defibrillation efficacy: a simulation study. Ann Biomed Eng (2008). , 36, 1659-67.

[35] Aguel, F, Eason, J. C, Trayanova, N. A, Siekas, G, & Fishler, M. G. Impact of transvenous lead position on active-can ICD defibrillation: a computer simulation study. Pacing Clin Electrophysiol (1999). , 22, 158-64.

[36] Witkowski, F. X, Penkoske, P. A, & Plonsey, R. Mechanism of cardiac defibrillation in open-chest dogs with unipolar DC-coupled simultaneous activation and shock potential recordings. Circulation (1990). , 82, 244-60.

[37] Geddes, L. A, Tacker, W. A, Rosborough, J. P, Moore, A. G, & Cabler, P. S. Electrical dose for ventricular defibrillation of large and small animals using precordial electrodes. J Clin Invest (1974). , 53, 310-9.

[38] Kroll, M. W, & Schwab, J. O. Achieving low defibrillation thresholds at implant: pharmacological influences, RV coil polarity and position, SVC coil usage and positioning, pulse width settings, and the azygous vein. Fundam Clin Pharmacol (2010). , 24, 561-73.

[39] Usui, M, & Walcott, G. P. KenKnight BH, et al. Influence of malpositioned transvenous leads on defibrillation efficacy with and without a subcutaneous array electrode. Pacing Clin Electrophysiol (1995). , 18, 2008-16.

[40] Crossley, G. H, Boyce, K, Roelke, M, et al. A prospective randomized trial of defibrillation thresholds from the right ventricular outflow tract and the right ventricular apex. Pacing Clin Electrophysiol (2009). , 32, 166-71.

[41] Mollerus, M, Lipinski, M, & Munger, T. A randomized comparison of defibrillation thresholds in the right ventricular outflow tract versus right ventricular apex. J Interv Card Electrophysiol (2008). , 22, 221-5.

[42] Turakhia, M, Prasad, M, Olgin, J, et al. Rates and severity of perforation from implantable cardioverter-defibrillator leads: a 4-year study. J Interv Card Electrophysiol (2009). , 24, 47-52.

[43] Swerdlow, C. D, Davie, S, Ahern, T, & Chen, P. S. Comparative reproducibility of defibrillation threshold and upper limit of vulnerability. Pacing Clin Electrophysiol (1996). , 19, 2103-11.

[44] Efimov, I. R, Cheng, Y, Yamanouchi, Y, & Tchou, P. J. Direct evidence of the role of virtual electrode-induced phase singularity in success and failure of defibrillation. J Cardiovasc Electrophysiol (2000). , 11, 861-8.

[45] Kroll, M. W. A minimal model of the single capacitor biphasic defibrillation waveform. Pacing Clin Electrophysiol (1994). , 17, 1782-92.

[46] Gold, M, Val-mejias, J, Leman, R. B, et al. Optimization of superior vena cava coil position and usage for transvenous defibrillation. Heart Rhythm (2008). , 5, 394-9.

[47] Jolley, M, Stinstra, J, Tate, J, et al. Finite element modeling of subcutaneous implantable defibrillator electrodes in an adult torso. Heart Rhythm (2010). , 7, 692-8.

[48] Lieberman, R, Havel, W. J, Rashba, E, Degroot, P. J, Stromberg, K, & Shorofsky, S. R. Acute defibrillation performance of a novel, non-transvenous shock pathway in adult ICD indicated patients. Heart Rhythm (2008). , 5, 28-34.